Nuclear Instruments and Methods in Physics Research A288 (1990) 379–388
North-Holland

MEASUREMENT OF THE INCLUSIVE p–C ANALYZING POWER AND CROSS SECTION IN THE 1 GeV REGION AND CALIBRATION OF THE NEW POLARIMETER POMME

B. BONIN, A. BOUDARD, H. FANET, R.W. FERGERSON *, M. GARÇON, C. GIORGETTI, J. HABAULT, J. LE MEUR, R.M. LOMBARD, J.C. LUGOL, B. MAYER, J.P. MOULY and E. TOMASI-GUSTAFSSON

Service de Physique Nucléaire à Moyenne Energie, CEN Saclay, 91191 Gif-sur-Yvette Cedex, France

J.C. DUCHAZEAUBENEIX and J. YONNET

LNS, CEN Saclay, 91191 Gif-sur-Yvette Cedex, France

M. MORLET, J. VAN DE WIELE and A. WILLIS

IPN-Orsay, Université de Paris-Sud, 91400 Orsay, France

G. GREENIAUS

Department of Physics, University of Alberta, Edmonton, Canada T6G 2J1 and TRIUMF, 4004 Wesbrook Mall, Vancouver, BC, Canada V6T 2A3

G. GAILLARD

Institut de Physique, Université de Genève, CH-1211 Genève 4, Switzerland

P. MARKOWITZ and C.F. PERDRISAT

College of William and Mary, Department of Physics, Williamsburg, VA 23185, USA

R. ABEGG and D.A. HUTCHEON

TRIUMF, 4004 Wesbrook Mall, Vancouver, BC, Canada V6T 2A3

Received 15 September 1989

We describe the polarimeter POMME, and give the results of its calibration in the region 200–1200 MeV, using the Saturne polarized proton beam. The high energy part of this domain (800–1200 MeV) was previously unexplored. Parametrizations of the inclusive p–C analyzing power and polarimeter efficiency as a function of scattering angle and incident energy are given, completing the data already available at lower energies. The optimization of proton polarimeters in this energy domain is also discussed.

1. Introduction

Nuclear physics with polarized probes is an ever growing field. As a natural consequence, the need for efficient and accurate polarimeters also increases. In order to meet these requirements at the Saturne facility, a large polarimeter has been built to measure both proton and deuteron polarization on the focal plane of a spectrometer. We report here the results of its calibration with the Saturne polarized proton beam in the region 200–1200 MeV. The high energy part of this domain had not been explored previously. In the first part of the paper, we describe briefly the apparatus (with emphasis on our special wire chamber readout system), and the calibration method; the second and third parts are devoted respectively to parametrizations of the inclusive p–C analyzing powers and polarimeter efficiency as a function of scattering angle and incident momentum. Parametrizations of the analyzing powers already exist up to 750 MeV. Our purpose is to comple-

* Permanent address: Rutgers University, Piscataway, New Jersey 08854, USA.

0168-9002/90/$03.50

ment these data at higher energy. In the last section, we discuss the figure of merit of proton polarimeters and their optimization.

The calibration of the same polarimeter with polarized deuteron beams is presented in the next article in this issue.

2. Experimental method

2.1. The apparatus

Polarimeters for medium energy protons are usually based on the small angle inclusive proton scattering on thick carbon targets. This principle is well known and documented [1–8], and many polarimeters using it already exist at Argonne [5], CERN [6], SIN [4,7], TRIUMF [3] and LAMPF [1,2]. In order to facilitate its use in various experimental environments, POMME (Polarimètre mobile à moyenne énergie) has been designed as a compact, movable, independent detection system, able to measure proton polarization in a large energy domain, and of a size sufficient to cover the entire focal plane of a typical medium energy magnetic spectrometer. The geometry of the polarimeter is summarized in fig. 1. The X and Y multiwire proportional chambers C_1, C_2, C_3 and C_4, C_5, C_6 permit the trajectory reconstruction of the particles respectively upstream and downstream of the carbon block, and so give the measurement of the scattering angles. The redundancy of the localization for each track allows a good control of the alignments. The sensitive area of the chambers is 50×50 cm^2 for C_1, C_2, C_3 and 100×100 cm^2 for C_4, C_5, C_6. The maximum angular range covered by the detection system is 0–30° for the scattered particle. The principle of readout of these chambers is somewhat uncommon and is described in the following section.

The carbon block consists of layers 1.2 or 2.4 cm thick which can be stacked to the desired thickness. The carbon density was 1.7 g/cm^3. The trigger is made with a coincidence of three plastic scintillator planes: P_1, P_2, ($0.5 \times 17 \times 50$ cm) and the 4 times $1.0 \times 26 \times 100$ cm hodoscoped wall Q. All the scintillators are viewed at both ends by a photomultiplier. About 90% of the events incoming on the C target undergo only multiple Coulomb scattering and are therefore useless for polarimetry purposes. A fast (100 μs) software rejection of these events is performed prior to the normal analysis. For simplicity the multitrack events are also rejected.

By setting windows on the longitudinal position of the vertex and on the minimum distance between the incoming and outgoing trajectories, the rescattered trajectories which lead to biased values of the polar (θ) and azimuthal (ϕ) angles can be rejected.

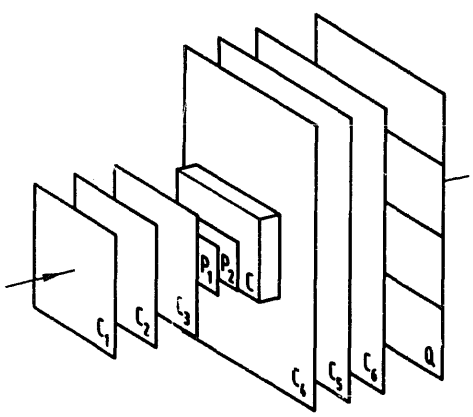

Fig. 1. The polarimeter POMME.

2.2. The wire chambers and their readout system

POMME-like polarimeters require a very careful and unbiased measurement of the polar and azimuthal scattering angles in the carbon block. This implies a precise alignment of the detectors and a stable track position measurement. Multiwire proportional chambers are attractive detectors for polarimetry, because they meet this stability requirement (no calibration of drift velocity), and because of their reliability and simplicity. The multiwire proportional chambers in POMME have a very classical design: the wire spacing is 2 mm, the gap is 4 mm for the small chambers and 6 mm for the large ones. The wires are gold-plated tungsten, 20 μm in diameter. We used a "magic gas" mixture with 70% Ar, 24% isobutane, 0.4% freon and 6% methylal. For an operating voltage of 2950 V (3850 V) the charge collected on the wire for a minimum ionizing proton was of the order of 0.7 pC (0.5 pC) with a dispersion of 0.35 pC (0.25 pC) FWHM on the small and large chambers respectively. For the sake of simplicity, the signal was taken on the anode wires.

POMME has been equipped with a simple, cheap and compact electronic chain to treat the wire chamber signal. POMME being designed to measure only one single track, a wire to wire electronic readout of the chambers seemed to be both unnecessary and expensive. Instead, a method of charge division was employed (fig. 2). The charge collected on the hit wire flows in a resistive line connecting all the anode wires. Charge preamplifiers regularly spaced along this resistive line amplify the charge [9]. The signal from each preamplifier is sent on a "receiver" which completes the amplification and transforms the signal into an unipolar shape in each channel. A fast ADC (LeCroy FERA) codes the charge. The information is then sent to the computer (SAR system [10]) via a CAMAC bus. Only the charge values above a chosen threshold are transmitted to the computer.

The collection of wires contained between two adjacent preamplifiers will hereafter be called a section. The

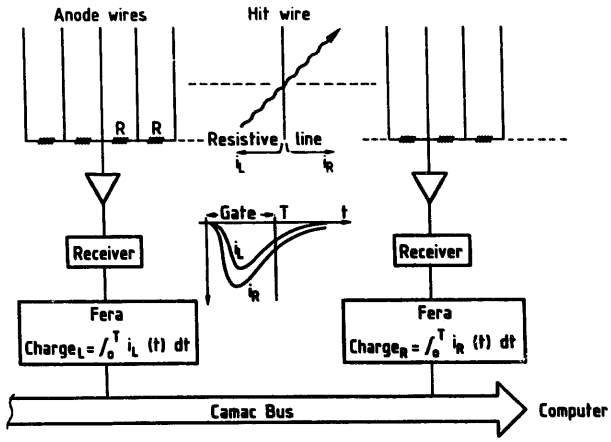

Fig. 2. Readout of the wire chambers.

three crucial parameters of this system are the spacing of the measurement channels (given by N_w, number of wires contained in one section), the interwire resistance R of the line, and the gate width T of the ADCs. Many constraints contribute to the choice of these parameters, including the cost of the electronics, the thermal noise in the interwire resistors, its influence on the resolution of the track localization, and the ability of the system to work in a high background environment. A large value for N_w reduces the number of measurement channels and hence the cost of the electronics. This is of course detrimental to the precision of the track localization. The thermal noise in the interwire resistor R degrades the information on the left and right charge measurements, and, consequently, on the track localization. This constraint prevents the use of small values for R. But high values for R lead to a large integration of the signal in the RC line of measurement. The gate width T has then to be enlarged to measure a significant charge. On the other hand, a small gate width T reduces the contribution of the thermal noise to the charge measurements. Furthermore, it is not necessary to extend the gate width so as to measure the totality of the charge: since the track localization will be obtained by a ratio of charge measurements (see eq. (1)), it is only necessary to measure the same proportion of the charge flowing in the left and right channels. POMME will have to work in environments with high counting rates. It is desirable to have narrow gates for the encoding of the charge, in order to minimize both the accidental event rate and the background contribution to the charge measurement.

The estimated background led us to choose a gate width $T = 100$ ns. For economic reasons, the number of electronic channels was chosen to be 16 per plane. Consequently, each section contains $N_w = 16$ wires for the small chambers, and 32 wires for the large ones. The choice for the interwire resistance value $R = 50\ \Omega$ for the small chambers and, $R = 25\ \Omega$ for the large ones comes from the above mentioned compromise. More details on the readout system will be given in a forthcoming paper.

With this choice of parameters, an electronic resolution of 0.3 mm and 0.8 mm for the small and large chambers respectively could be achieved for a charge of 1 pC delivered on the wire.

The position x of the hit wire inside a section bordering the preamplifiers (left) L and (right) R was given by the formula

$$x = f(t + nt^3), \tag{1}$$

where

$$t = \frac{r \times \text{charge R} - \text{charge L}}{r \times \text{charge R} + \text{charge L}}.$$

The parameter r is the relative gain of the left-to-right electronic channel and is about 1. The value of r was determined with a precision of 3% by injecting a generator signal at the middle of each section and was adjusted finely by ensuring, with particles, that the central wire did appear in the exact middle of the section (fig. 3); the effective parameters f and n (whose values are respectively about 1 and 0) were introduced in order to account for slight nonlinearities in the charge division and small cross-talk between adjacent ADCs. There are only four f and n parameters, i.e. one of each kind for the small and large chambers. Their values were adjusted empirically so as to obtain track position spectra

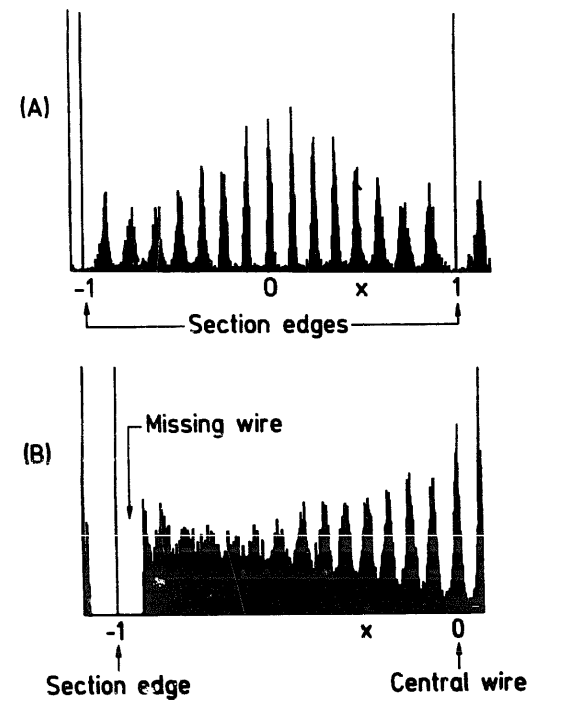

Fig. 3. Position spectrum obtained by a uniform illumination of a small (A) and large (B) wire chamber from POMME. A whole section is displayed in (A); only half a section is shown in (B). In both cases, the resolution is good enough to enable the determination of the hit wire.

which give the reconstructed wire location with the correct 2-mm spacing (fig. 3).

When the hit wire is close to a section edge, there is a strong asymmetry between the charge collected on the right and on the left side of the section. On the large chambers, it may even happen that the charge flowing on the far side is of the same order of magnitude as the electronic noise, and does not pass the ADC threshold. In this case, only the near side ADC is hit, and the charge division information is lost. This causes a loss of precision for the localization of the tracks close to the section edges. This systematic error affects one wire adjacent to the section edge on the large chamber (2-mm error). On the small chambers, the signal-to-noise ratio of the charge division is more favourable, and charges collected on the right and on the left of the section pass the ADC threshold wherever the hit wire is. The position spectrum is thus unaffected by this systematic error. In spite of this loss of information near the section edges, the resolution of the wire chambers is acceptable. It can be estimated from the width of the alignment spectrum: for a uniform illumination of the chambers, the extracted resolution is 2.8 and 3.2 mm FWHM for the small and large chambers respectively. These values, which are still dominated by the wire spacing (2 mm), permit sufficient accuracy in the determination of the polar and azimuthal scattering angle θ and ϕ: the average FWHM error on θ is 0.18°, and the error on ϕ is 1° for a polar scattering angle of $\theta = 10°$. The efficiency of detection of one plane is 98% for minimum ionizing protons.

2.3. The Monte Carlo simulation

A complete Monte Carlo (MC) simulation of an event in POMME was done for proton energies up to 800 MeV, in order to gain understanding on its behaviour prior to the calibration.

The event simulation proceeded as follows: a polarized proton crosses the first three chambers, and hits the carbon block. Three possible reactions are then considered: multiple Coulomb scattering, nuclear absorption, and the useful p–C elastic or quasi-elastic scattering. The corresponding cross sections were not a priori available (except the useful p–C quasi-elastic scattering angular distribution, given without normalization in ref. [7], and were guessed on a reasonable basis, thus giving the probability law for the random variable θ (polar scattering angle). The probability law for ϕ involves the knowledge of the inclusive p–C analyzing powers, which was assumed to be zero in the case of multiple Coulomb scattering, and taken from McNaughton's parametrization [1] in the case of p–C quasi-elastic scattering. The slowing down of the proton in a thick C target was taken into account, as well as the possibility of a second collision. Straggling in the air and in the detectors (of finite resolution) were considered and the process of noise generation and charge division in the wire chambers readout system was also simulated.

The above described MC simulation turned out to be a very useful and predictive tool. It gave us precious hints on the bias brought up by systematic or random errors on the track reconstruction. We could check the effect of misalignments of the detectors, and determine the minimum resolution required for a proper operation of POMME, In particular, the MC simulation enabled us to check that the systematic error due to the loss of one wire close to the section edge in the large wire chambers would not introduce serious bias on the analyzing powers measured by POMME during its calibration, or on the polarization measured by the calibrated polarimeter.

The MC simulation also predicted that the p–C inclusive analyzing powers should depend strongly on the carbon thickness. We used it to gain information on the best carbon thickness and minimum scattering angle to be used for an optimum operation of POMME. The MC predictions were entirely confirmed by the subsequent calibration.

2.4. Measurement method

At each proton energy, there must exist an optimum thickness for the C target, maximizing the figure of merit of the polarimeter. The definition of the figure of merit, and the reasons for the existence of an optimum will be discussed in detail in section 5. We calibrated POMME close to this optimum, and gained information on its location by using at least two C thicknesses at each proton energy (see table 1).

The measurements were performed directly in the polarized beam delivered by the synchrotron Saturne, without any scattering in a primary target. The polarization P of the incident beam was about 90% at 500 MeV, and 80% at 1200 MeV. This polarization was monitored continuously by a beam line polarimeter based on the proton elastic scattering on a CH_2 target [11]. The statistical error on P was lower than 0.1%, and was neglected. The systematic error was estimated to be 2%.

The spin orientation of the incoming protons was reversed for every burst, thus allowing a reliable check for the absence of instrumental asymmetries. The analyzing powers were extracted as follows: for each spin orientation of the incident beam, a bidimensional spectrum (θ, ϕ) was constructed, summarizing all the information available from the polarimeter. After suitable normalization of these spectra by the incident beam intensity and dead time, the content of the spectra can

Table 1
Incident energies for the calibration of POMME, and the corresponding carbon thicknesses. The density of the graphite used was 1.7 g/cm^3. The data sets forming the data base for the parametrization discussed in this paper are underlined.

T_{inc} [GeV]	e_C [cm]
0.200	4.8
	7.2
	9.6
	12.0
0.500	7.2
	12.0
	24.0
	31.2
0.800	21.6
	31.2
1.050	21.6
	31.2
1.200	21.6
	30.0

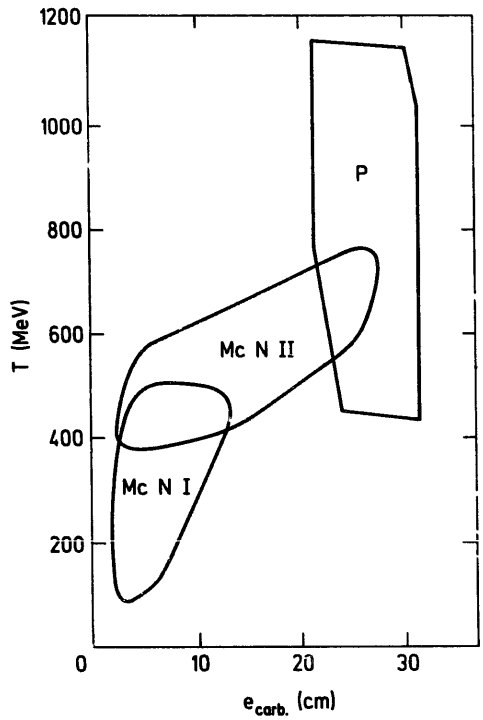

Fig. 4. Validity domain for the various parametrizations of the inclusive p–C analyzing power. T is the lab. proton energy at the carbon center. The validity domain of the two McNaughton's parametrizations have been extracted from the fitting data base of ref. [1].

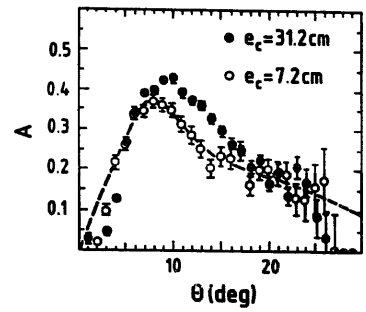

Fig. 5. Comparison of the McNaughton's parametrization at 500 MeV (dashed line) with our experimental data for two different carbon thickness values.

be written as:

$$N^{\pm}(\theta, \phi) = C\frac{d\sigma}{d\Omega}(\theta)D(\theta, \phi)(1 \pm PA(\theta)\cos\phi),$$

where $A(\theta)$ is the analyzing power of the reaction, $D(\theta, \phi)$ is the detection efficiency of the polarimeter in the (θ, ϕ) region, C is a constant, and the $\pm$ sign refers to the spin orientation of the incident protons.

The determination of the analyzing power $A(\theta)$ proceeds by calculating the ratio

$$R_v(\theta, \phi) = \frac{N^+ - N^-}{N^+ + N^-} = PA(\theta)\cos\phi,$$

thus getting rid of the detection efficiency $D(\theta, \phi)$.

A fitting procedure then calculates $PA(\theta)$ from $R_v(\theta, \phi)$, and finally $A(\theta)$, knowing P. The χ^2 of the fit is an indication on the validity of the procedure. In our case, the χ^2 value was always less than 1.5.

For a good polarimeter, the function $D(\theta, \phi)$ has to be independent of ϕ. We could prove that this was indeed the case in the whole acceptance domain of POMME, since quantity

$$N^+ + N^- = 2C\frac{d\sigma}{d\Omega}(\theta)D(\theta, \phi)$$

could be fitted by a constant independent of ϕ with a χ^2 smaller than 1.5 in all θ bins for $4.5° < \theta < 18.5°$.

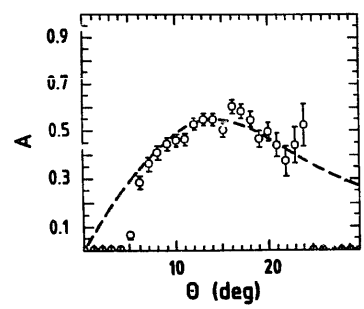

Fig. 6. Comparison of the McNaughton's parametrization (dashed line) and our calibration data points at 200 MeV for e_c = 7.2 cm.

3. The analyzing power

POMME has been calibrated at 200, 500, 800, 1050 and 1200 MeV. The measurement at 200 MeV was done in order to check our experimental setup and make an overlap with the McNaughton's parametrization [1] (table 1).

At 500 MeV, a Monte Carlo simulation, performed prior to the experiment predicted an optimum for the figure of merit for a very large carbon thickness, never used so far in any polarimeter. We therefore checked this prediction and calibrated POMME around this optimum.

At 1050 and 1200 MeV, no calibration data were available in the literature.

The analyzing power data obtained are shown in figs. 5, 6 and 7. Between 500 GeV and 800 MeV, the average analyzing power first decreases sharply, and levels off at higher energy, at a value of about 0.2. At 800 MeV and above, this value is obtained for scattering angles as small as 5°, where the cross section is large. The analyzing power behaves very smoothly as a function of angle in the whole studied angular domain. These features permit to establish on firm grounds the feasibility of proton polarimeters in the GeV region. It is thus useful to have a parametrization of the analyzing power for polarimetry applications in this energy range.

3.1. Parametrization

The parametrization given here is valid between 500 and 1200 MeV and extends to higher energy the existing data, with an overlap with the last parametrization of McNaughton et al. [1] which extends up to 750 MeV (fig. 4). For convenience, we have used the same analytical form as McNaughton (at high energy) for our parametrization of the inclusive p–C analyzing powers:

$$A(\theta\ p) = \frac{ar}{1 + br^2 + cr^4} + dp\ \sin(5\theta),$$

with $r = p\ \sin(\theta)$, where p is the proton momentum at the carbon center in GeV/c. The quantities a, b, c, d are parametrized as a function of p in the following way:

$$a = a_0 + a_1 p' + a_2 p'^2 + a_3 p'^3,$$

$$b = b_0 + b_1 p' + b_2 p'^2 + b_3 p'^3,$$

$$c = c_0 + c_1 p' + c_2 p'^2 + c_3 p'^3,$$

$$d = d_0 + d_1 p' + d_2 p'^2 + d_3 p'^3,$$

where the shift

$$p' = p - 1.4\ \text{GeV}/c$$

has been made in order to handle a variable centered around zero in our parametrization domain, and to obtain a stable behaviour of the parametrization outside this domain.

3.2. Thickness dependence of A

The above parametrization does not depend explicitly on the carbon thickness. But, since p is the average momentum at the center of the block, it is assumed that the thickness dependence reduces to an energy dependence accounting for the energy loss in the block. Due to straggling effects, this assumption is certainly wrong for large thicknesses.

However, the quality of the obtained fit proves that this assumption is valid for the limited C thickness range we have investigated, close to the optimum for the figure of merit. The parametrization should thus be sufficient for polarimetry applications. As will be shown in section 5, it turns out that the figure of merit is reasonably close to its optimum if a constant C thickness of about 30 cm is used in the whole energy range between 500 and 1200 MeV. The parametrization we give is valid in a C thickness domain between 20 and 31 cm. It includes all effects of straggling and energy loss in the C block. It should be noted that in the domain of overlap between McNaughton's parametrization and ours (i.e. 500–750 MeV), the analyzing powers depend rather strongly on the carbon thickness (fig. 5).

POMME has also been calibrated at 500 MeV with smaller carbon thickness: 7.2 and 12 cm. Data are then fitted correctly by the McNaughton's parametrization (fig. 5). However, we considered that this thickness was too far from the optimum, and the corresponding data points were not included in the data base for our own parametrization.

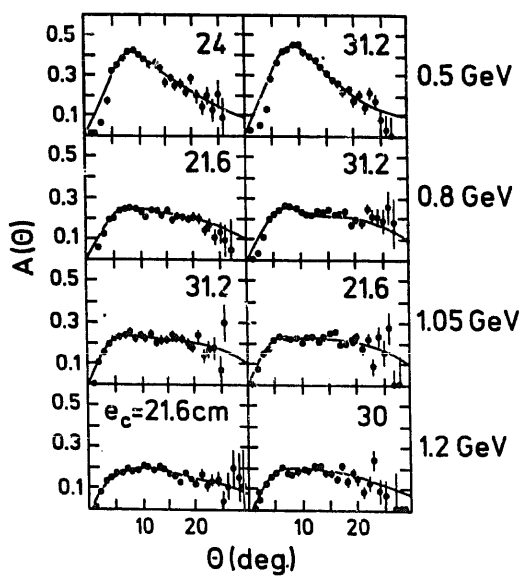

Fig. 7. Global fit of the analyzing power data for various values of the carbon thickness e_c (in cm) and incident energy (in GeV).

Table 2
Best fit parameters of the inclusive p–C analyzing power parametrization.

	0	1	2	3
a	1.626 ± 0.29	−1.786± 0.80	1.933± 1 85	−0.285± 4.14
b	14.909 ± 7.17	−0.594± 0.32	−91.766± 65.66	207.064± 96.45
c	574.719 ±54.44	−560.410±408.40	−610.026±1154.7	−1154.66 ±2257.8
d	0.1275± 0.022	0.055± 0.062	−0.138± 0.14	−0.639± 0.31

At 200 MeV, the best figure of merit is obtained for a carbon thickness of 7.2 cm. This value has been widely used for existing polarimeters, and is located in the validity domain of McNaughton's parametrization. The agreement between our calibration data and this parametrization is excellent (fig. 5). For the energy region 500–1200 MeV, the best fit parameters and their errors are summarized in table 2. The best fit has been made on eight calibration data sets, at 500, 800, 1050 and 1200 MeV, with two C thicknesses for each energy and for scattering angles between 4.5° and 26.5° (see table 1). The global χ^2 of the fit is 1.25 per data point. As can be seen on fig. 7, the visual agreement of the fit is quite satisfactory in the angular range of interest, with no systematic trends.

4. Parametrization of the polarimeter efficiency

The differential efficiency $\epsilon(\theta)$ of a polarimeter is usually defined as

$$\epsilon(\theta)\,\mathrm{d}\theta = \frac{N_u(\theta)}{N_{inc}}\mathrm{d}\eta,$$

where $N_u(\theta)\,\mathrm{d}\theta$ is the number of usefully scattered particles in the angular bin $(\theta, \mathrm{d}\theta)$, and N_{inc} is the total number of particles incoming on the polarimeter. $\epsilon(\theta)$ depends of course on the carbon thickness e_C and proton momentum p.

As a by-product of the calibration of POMME, we could measure $\epsilon(\theta)$ with good precision, since the incident beam was counted particle per particle. The detection efficiency was determined with an accuracy of 5% by a majority coincidence method, used separately for the front and rear chambers. This gives the precision of the normalization of ϵ. It should be noted that the

$$p + C \rightarrow 1 \text{ charged particle} + X$$

yield we have measured is probably very close to the inclusive C(p, p′)X yield for two reasons:

i) the cross sections for C(p, $\pi^{\pm}$)X, C(p, d)X, C(p, ^{3}He)X, etc are certainly negligible as compared with C(p, p′)X,

ii) we could check that the proportion of $p + C \rightarrow 2$ charged particles or more + X events was less than 5% in all the angular acceptance domain of POMME and for all the studied incident energies.We give here a parametrization of the polarimeter efficiency ϵ as a function of the lab scattering angle θ, the carbon thickness e_C, and the proton momentum at the carbon center p. This parametrization could be useful for various counting rate estimates. We assumed the following analytical form in the laboratory system:

$$\epsilon(\theta, e_c, p) = 2\pi \sin\theta \times \frac{\pi}{180}\left(\frac{e_C \rho_C N_A}{12}\right) \times e^{-e_C/L(p)}\left[G(p)\, e^{B\theta + C\theta^2 + D\theta^3}\right]$$

where ρ_c is the density of the C target (1.7 g/cm^2) and

Table 3
Best fit parameters for our inclusive p–C differential efficiency parametrization. Units are deg^{-1} for $E(\theta)$, degrees for θ, cm for e_C and GeV/c for p.

	0	1	2
B	-0.880×10^{-0}		
C	0.567×10^{-1}		
D	-0.139×10^{-2}		
G	-0.298×10^{-22}	0.932×10^{-22}	-0.0239×10^{-22}
L	0.353×10^{2}	-0.158×10^{1}	-0.262×10^{-2}

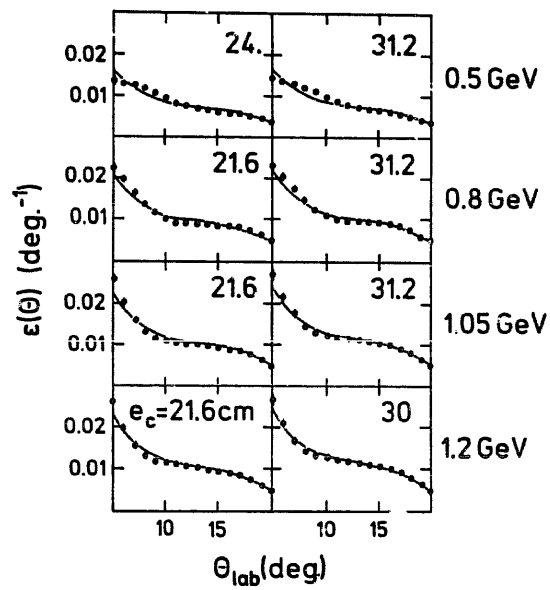

Fig. 8. Global fit of the yield data for various values of the carbon thickness e_C (in cm) and incident energy (in GeV).

N_A the Avogadro number. We assumed a polynomial dependence of the quantities G and L as a function of p:

$$G(p) = G_0 + G_1 p + G_2 p^2,$$

$$L(p) = L_0 + L_1 p + L_2 p^2.$$

The data base for the determination of the best fit parameters B, C, D, G_i, L_i was the same as for the analyzing power parametrization, but limited to $\theta < 19°$. The values obtained are summarized in table 3, and the quality of the fit is shown in fig. 8. The validity domain of the parametrization is as follows:

$1.0 < p < 1.9$ GeV/c

$4.5° < \theta < 18.5°$

$20 \leq e_c \leq 31$ cm.

This domain is probably somewhat wider due to the very smooth behaviour of the yield. The average agreement with the experimental data is better than 8%.

The main thickness dependence of the yield is constrained in the $\exp(-e_C/L(p))$ term which describes the attenuation of the proton flux in the block. As can be seen in fig. 8, this thickness dependence describes correctly the experiment, thus suggesting that $L(p)$ corresponds more or less to a physical attenuation length associated with all processes giving 0 or >1 detected particles in the final state. For 800-MeV protons, $L(p) = 35$ cm; the cross section corresponding to this attenuation length is 285 mb, a result close to the geometrical p–C cross section

$$\sigma_{geom} = \pi R_C^2 = 280 \text{ mb}$$

determined from a strong absorption model with an interaction radius of 3 fm. The analytical form chosen for our parametrization is thus justified from a physical point of view.

5. Optimization

5.1. Optimum thickness for the C target

For a POMME-type proton polarimeter, increasing the thickness of the C target has many consequences:

– The probability of a useful p–C interaction increases, at least for reasonably small C thicknesses.

– The probability of a parasitic p–C reaction also increases. This can be viewed as a loss of flux for the incoming and outgoing proton.

– The multiple Coulomb scattering in the block increases and the multiple scattering cone overlaps the useful nuclear p–C scattering at small angles, thus reducing the effective analyzing power in the small angle region.

– Due to the energy loss in the C block, the average energy of the p–C interactions decreases, thus modifying the (strongly energy-dependent) effective p–C analyzing power.

The competition between all these effects results in an optimum thickness for the C block. After having parametrized the analyzing power $A(\theta, e_C, p)$ and the polarimeter efficiency $\epsilon(\theta, e_C, p)$, it becomes possible to evaluate the performance of a POMME-type polarimeter for various incident energies and carbon thickness, and to optimize it as a function of e_C.

The statistical error on the polarization P of N_{inc} incoming particles is given by

$$\Delta P = \frac{\sqrt{2}}{F\sqrt{N_{inc}}},$$

where the constant F is a quantity characteristic of the polarimeter, called the figure of merit.

For a POMME-type polarimeter, one has

$$F^2 = \int_{\theta_{min}}^{\theta_{max}} A(\theta)^2 \epsilon(\theta)\, d\theta,$$

where $(\theta_{min}, \theta_{max})$ defines the scattering angle domain taken into account for the calculation of the polarization. We have calculated this integral in a realistic polarimeter case by taking $\theta_{min} = 4.5°$ and $\theta_{max} = 18.5°$. This value of θ_{min} was chosen because it excludes the multiple scattering cone from the useful solid angle of the polarimeter for all carbon thickness considered here, and because $\theta_{min} = 4.5°$ is the smallest scattering angle practically measurable on POMME without bias on the azimuthal scattering angle ϕ. The value $\theta_{max} = 18.5°$ was chosen because it is the maximum scattering angle with a uniform azimuthal acceptance on POMME.

In order to investigate the location of the optimum for the figure of merit, the calculation of F^2 has been performed for various carbon thickness in the range $e_C = 15$–35 cm. This range is slightly wider than the validity domain of our parametrization for A and ϵ, but the smooth behaviour of these parametrizations should nonetheless enable us to draw reasonable conclusions.

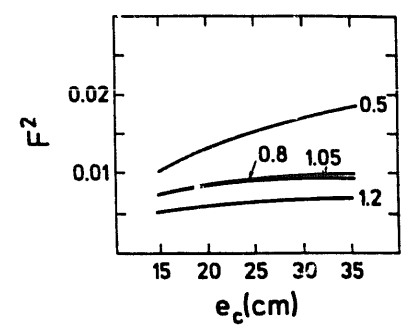

Fig. 9. Figure of merit (squared) of a POMME-like proton polarimeter, as a function of the carbon thickness and for various incident energies (in GeV).

The resulting figure of merit is shown in fig. 9 as a function of e_C for various incident energies. It appears that the 30-cm thickness data sets are quite close to the calculated optimum at all energies. At 500 MeV, the optimum for the figure of merit is not yet reached for a C thickness of ~ 30 cm, i.e. about twice as much as the currently-used thicknesses. The gain in figure of merit is substantial, so this result should have practical consequences. Here, the C block plays the role of a degrader, in an energy region, where the analyzing power grows strongly when the energy decreases (fig. 7). Between 800 and 1200 MeV, the figure of merit decreases very little, thus suggesting that proton polarization measurements will be still feasible with the same principle at even higher energies.

5.2. Average analyzing power and efficiency

The performance of a polarimeter is not characterized by its figure of merit only, but also by its average analyzing power $\bar{A}$: whereas the figure of merit determines the statistical error on P, the magnitude of $\bar{A}$ determines to a large extent the systematical error on P.

$\bar{A}$ is defined as

$$\bar{A} = \frac{F}{\sqrt{\epsilon}},$$

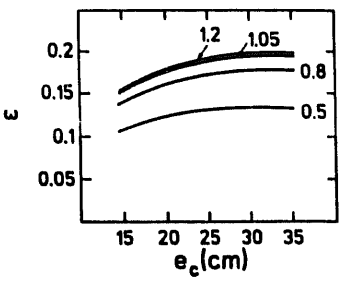

Fig. 10. Efficiency of a POMME-like proton polarimeter, as a function of the carbon thickness and for various incident energies (in GeV).

where ϵ is the global efficiency of the polarimeter:

$$\epsilon = \int_{\theta_{min}}^{\theta_{max}} \epsilon(\theta)\, d\theta.$$

We have computed ϵ within the same angular limits as F. the result for ϵ and $\bar{A}$ is plotted in figs. 10 and 11 for various incident energies as a function of e_c.

It can be seen from these figures that the carbon thickness we propose (around 30 cm) corresponds to rather large average analyzing powers (in any case, not smaller than for smaller C thicknesses) and that this value is usable in practice, since the minimization of the statistical error on P has not been done at the expense of the systematic error.

5.3. Angular domain

It is also interesting to study the differential quantity

$$g(\theta) = A(\theta)^2 \epsilon(\theta),$$

because $g(\theta)\,\Delta\theta$ represents the contribution to the global figure of merit of the angular region $\Delta\theta$ centered around θ. The curve $g(\theta)$ is plotted as a function of θ for a 30-cm C thickness and for various energies (fig. 12). The domain where $g(\theta)$ peaks is the interesting one for polarimetry applications. It becomes smaller and smaller as the energy increases, because the cross sections and analyzing power become more and more forward peaked. It can be seen from the fig. 12 that in the region 500–1200 MeV, it is almost useless to measure scattering angles beyond 15°. At these angles, the analyzing power reaches large values, but this advantage is offset by small cross sections. At small angles, the situation is opposite, since the large value of the cross section is compensated by the smallness of the analyzing power.

The net result is that one would not gain much in figure of merit by measuring angles as small as 4° (fig. 12). Anyway, the small analyzing powers and difficulty of correctly measuring ϕ at small scattering angles makes it difficult to get rid of systematic errors in this angular region. For the whole energy domain studied,

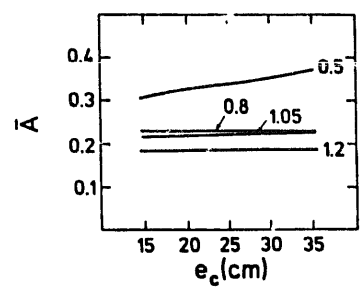

Fig. 11. Average analyzing power of a POMME-like proton polarimeter, as a function of the carbon thickness and for various incident energies (in GeV).

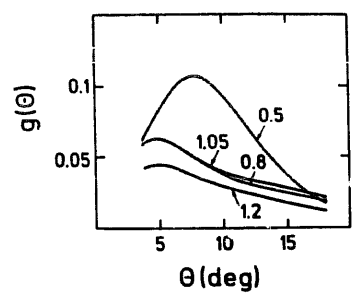

Fig. 12. Differential figure of merit $g(\theta)$ of a POMME-like proton polarimeter, for $e_C = 30$ cm and for various incident energies (in GeV).

the safest minimum scattering angle seems to be around 4.5°. This angle is larger than the aperture of the multiple scattering cone for all carbon thicknesses usable in practice. Therefore, the optimal carbon thickness is really governed by the maximum of $\bar{A}\sqrt{\epsilon}$, and not by multiple scattering considerations.

Acknowledgements

POMME has been built mainly by the Service de Physique Nucléaire à Moyenne Energie (DPhN/ME) at Saclay. Two of us (P.M. and C.F.P.) wish to acknowledge support from the National Science Foundation (NSF 88-11792). The participation of D.H., R.A. and G.G. was supported by grants from the National Sciences and Engineering Research Council of Canada, and by a NATO collaboration grant. We also acknowledge the CNRS for support, F. Lehar for his advice in the use of the beam line polarimeter, the Saturne staff for an excellent beam delivery during the calibration, and C. Glashausser and the Los Alamos HRS polarimeter team for useful contacts.

References

[1] M.W. McNaughton et al., Nucl. Instr. and Meth. A241 (1985) 435.
[2] R.D. Ransome et al., Nucl. Instr. and Meth. 201 (1982) 315.
[3] G. Waters et al., Nucl. Instr. and Meth. 153 (1978) 401; O. Hausser et al., Nucl. Instr. and Meth. A254 (1987) 67.
[4] D. Besset et al., Nucl. Instr. and Meth. 184 (1981) 365.
[5] G.W. Abshire et al., Phys. Rev. D12 (1975) 3393.
[6] D. Aebisher et al., Nucl. Instr. and Meth. 124 (1975) 49.
[7] E. Aprile-Giboni et al., Nucl. Instr. and Meth. 215 (1983) 147.
[8] D. Besset et al., Nucl. Instr. and Meth. 166 (1979) 379.
[9] R. Chaminade et al., Nucl. Instr. and Meth. 118 (1974) 477.
[10] B. Bricaud et al., IEEE Trans. Nucl. Sci. NS-26 (1979) 4641.
[11] J. Bystricky et al., Nucl. Instr. and Meth. A239 (1985) 31.